

*Citation for published version:*

Roscow, J, Bowen, C & Almond, D 2017, 'Breakdown in the case for materials with giant permittivity?', *ACS Energy Letters*, vol. 2, no. 10, pp. 2264-2269. <https://doi.org/10.1021/acsenergylett.7b00798>

*DOI:*

[10.1021/acsenergylett.7b00798](https://doi.org/10.1021/acsenergylett.7b00798)

*Publication date:*

2017

*Document Version*

Peer reviewed version

[Link to publication](#)

This document is the Accepted Manuscript version of a Published Work that appeared in final form in *ACS Energy Letters*, copyright © American Chemical Society after peer review and technical editing by the publisher. To access the final edited and published work see DOI: 10.1021/acsenergylett.7b00798.

## University of Bath

### Alternative formats

If you require this document in an alternative format, please contact:  
[openaccess@bath.ac.uk](mailto:openaccess@bath.ac.uk)

#### General rights

Copyright and moral rights for the publications made accessible in the public portal are retained by the authors and/or other copyright owners and it is a condition of accessing publications that users recognise and abide by the legal requirements associated with these rights.

#### Take down policy

If you believe that this document breaches copyright please contact us providing details, and we will remove access to the work immediately and investigate your claim.

# A Breakdown in the Case for Materials with Giant Permittivity?

J. I. Roscow<sup>1</sup>, C. R. Bowen<sup>1,\*</sup> and D. P. Almond<sup>1</sup>

<sup>1</sup> Materials and Structures Centre, Department of Mechanical Engineering, University of Bath, Bath, BA2 7AY.

\* Correspondence to: c.r.bowen@bath.ac.uk

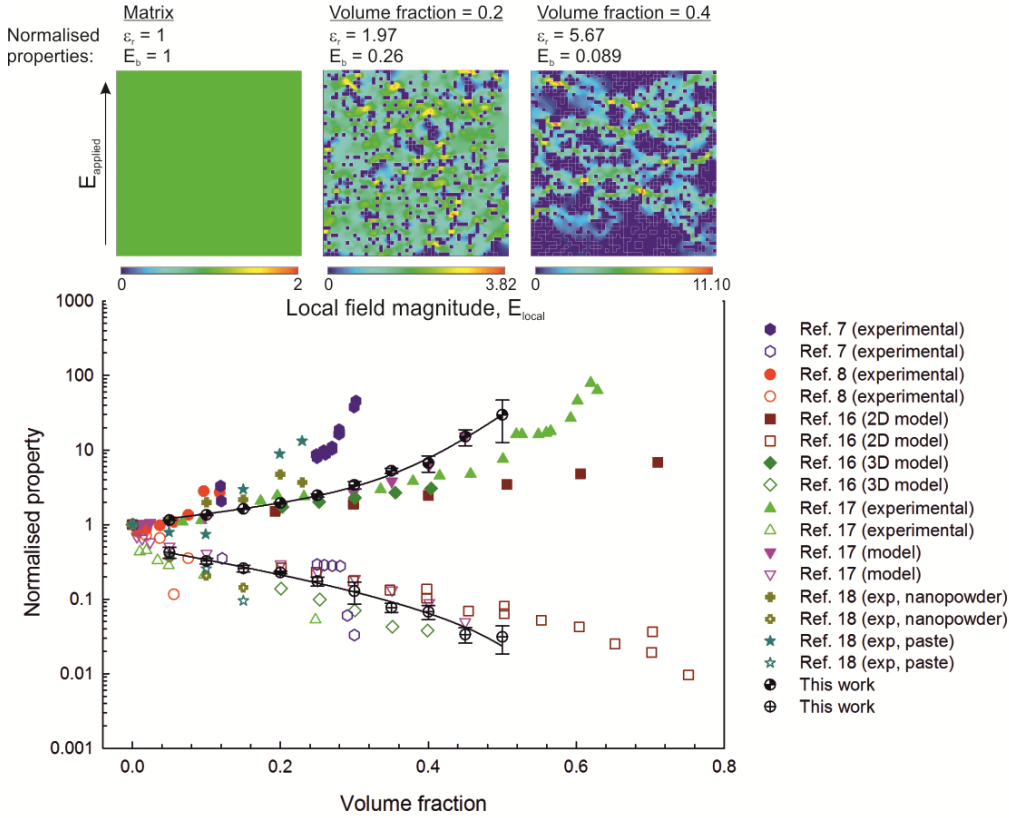


Fig. 1. Graph showing permittivity (solid symbols) and dielectric strength (open symbols) as a function of conductor volume fraction normalised to the single phase matrix material. The colour and symbol type is the same for the permittivity and dielectric strength for each system. Electric field contour plots are shown above the graph for increasing conductor volume fractions; an increase in local field concentrations with increasing conductor fraction leads to a rise in permittivity ( $\epsilon$ ) and decrease in breakdown strength ( $E_b$ ).

There remains continued interest in the design and manufacture of heterogeneous materials with high permittivity; for example the so-called ‘giant’ or ‘colossal’ permittivity materials. These materials can be divided into two distinct classes. The first class are ‘intrinsic’ giant permittivity materials in which the dipolar response of the material has been enhanced; for example doped titania materials.<sup>1-3</sup> The second class can be classified as ‘extrinsic’ where a high effective permittivity is achieved by introducing electrical conductivity or creating a composite system that consists of a dielectric matrix with a random or ordered distribution of a conductive filler.<sup>4</sup> Specific examples of extrinsic composites with high permittivity include metal-loaded ceramics (cermets) including Mo-mullite<sup>5</sup> and Ag-bismuth zinc niobate,<sup>6</sup> metal loaded ferroelectrics such as BaTiO<sub>3</sub>,<sup>7,8</sup> metal loaded glass<sup>9</sup> and metal-<sup>10</sup> and carbon-loaded<sup>11-13</sup> polymer matrices.

The reason for the interest in extrinsic materials is simple - the introduction of a conductive phase into a dielectric matrix creates a composite with an effective permittivity that is much higher than that of the matrix. Relative permittivity ( $\epsilon_r$ ) values of up to  $10^5$  have been reported in some composite systems. In many cases the permittivity and dielectric loss of the composite are characterised in detail, since the frequency dependent properties of materials are readily measured in the Hz to MHz range using frequency response analysers. It is common for publications related to the manufacture and characterisation of these high permittivity composites to highlight their potential application as multi-layer and small volume high-performance capacitors. However, while the permittivity and dielectric loss is of importance it is insufficient to fully assess their potential for such applications since the dielectric strength, or breakdown strength, is also an important parameter. The selection of materials for capacitor applications has been well described by McLean<sup>14</sup> and is summarised below for the design of capacitors with high reliability, low cost and small size.

For small volume capacitor applications it is necessary to use the smallest amount of dielectric to meet the capacitance requirements. Considering a simple parallel plate capacitor, the overall capacitance ( $C$ ) is,

$$C = \frac{A\epsilon_r\epsilon_0}{t} \quad \text{Eqn.1}$$

where  $A$  is the plate area,  $t$  is the plate separation (thickness),  $\epsilon_r$  is the relative permittivity of the dielectric medium and  $\epsilon_0$  is the permittivity of free space. The volume of the dielectric ( $V_{\text{dielectric}}$ ) is:

$$V_{\text{dielectric}} = A.t \quad \text{Eqn. 2}$$

From Eqns. 1 and 2 the capacitance per unit volume ( $\text{F m}^{-3}$ ) is therefore:

$$\frac{C}{V_{\text{dielectric}}} = \frac{\epsilon_r\epsilon_0}{t^2} \quad \text{Eqn. 3}$$

At this stage it is easy to assume that to achieve a high capacitance per unit volume a high permittivity is necessary, hence the interest in ‘giant’ permittivity materials. However, to maximise the capacitance per unit volume the thickness of the dielectric must also be as small. The minimum thickness is limited by the dielectric strength ( $E_{\text{dielectric}}$ ) of the capacitor material. If the capacitor has a working voltage,  $V$ , the minimum thickness is  $V/E_{\text{dielectric}}$ . Substituting this into Eqn. 3 leads to:

$$\frac{C}{V_{\text{dielectric}}} = \epsilon_r\epsilon_0 \left[ \frac{E_{\text{dielectric}}}{V} \right]^2 \quad \text{Eqn. 4}$$

Eqn. 4 shows that for a specific working voltage the capacitance per unit volume is proportional to a ‘merit index’ of  $\epsilon_r.(E_{dielectric})^2$ . This clearly highlights that a low dielectric strength can lead to poor volume efficiency, even if the permittivity is high. Rearrangement of Eqn. 4 also provides a figure of merit for a capacitor with high ‘energy density’ ( $J m^{-3}$ ). Since the energy stored in a capacitor is  $\frac{1}{2}CV^2$ , the ‘energy density’ is given by:

$$\frac{\frac{1}{2}CV^2}{V_{dielectric}} = \frac{1}{2}\epsilon_r\epsilon_0.(E_{dielectric})^2 \quad \text{Eqn. 5}$$

and leads to the same merit index of  $\epsilon_r.(E_{dielectric})^2$  for maximum energy density.

Eqns. 4 and 5 clearly show that *both* relative permittivity and dielectric strength are important parameters for the selection of a material for capacitor applications. The dielectric strength cannot be ignored when considering potential materials for capacitor applications. In fact, the  $\epsilon_r.(E_{dielectric})^2$  relationship in Eqn. 4 indicates that dielectric strength is a more important property than permittivity for high energy density capacitors. It is therefore of interest to now examine the influence of the addition of a conductive phase on the permittivity, the dielectric strength and the  $\epsilon_r.(E_{dielectric})^2$  merit index of a composite.

### Examples of extrinsic systems

Although a significant amount of data on frequency dependent permittivity and loss has been published on conductor-insulator composites and giant permittivity materials, there is much less data reporting both permittivity and dielectric strength. While the addition of a conductive filler increases the effective permittivity it can also have a deleterious effect on the dielectric strength as a result of the enhancement of local electric fields with the composite.<sup>11,15</sup> Gyure et al.<sup>16</sup> have modelled the dielectric breakdown and permittivity of metal-loaded dielectrics and Duxbury et al.<sup>17</sup> considered rocket propellant mixtures based on aluminium particles in a dielectric host that resulted in a significant reduction of the breakdown field of the host due to the presence of conductive aluminium particles. A variety of researchers have experimentally examined the dielectric strength and permittivity of Ni-BaTiO<sub>3</sub> composites.<sup>7,8,18</sup>

Fig. 1 shows a graph of normalised variation of permittivity (solid symbols) and dielectric strength (open symbols) as a function of conductor volume fraction for a range of composite systems from the literature<sup>7,8,16,17,18</sup> that contain experimental measurements or modelling data. To simplify a comparison, the colour and symbol is the same for both permittivity and dielectric strength for each composite. For the limited number of publications where both permittivity and dielectric strength were reported as a function of conductor volume fraction, Fig.1 clearly shows that the enhancement of permittivity is always at the expense of the dielectric strength.

It is now of benefit to calculate the  $\epsilon_r.(E_{dielectric})^2$  figure of merit as a function of conductor volume fraction for the data in the literature. For the data in Fig. 1, the permittivity and dielectric strength were not always available at the same conductor volume fractions; this was obtained by curve fitting of the data in Fig. 1 and calculating the relevant merit index across the range of volume fraction available for each data set.

The data fits were used to calculate the variation of normalised energy density figure of merit (Eqn. 5) with conductor volume fraction reported, as shown in Fig. 2. It can be seen that for all data, other than that reported by Pecharromán et al. (see supporting information),<sup>7</sup> the introduction of the conductor-phase leads to the figure of merit being reduced significantly compared to that of the filler free matrix, as the exponential rise in the permittivity coincides with a rapid reduction in the breakdown strength. The data reported by Pecharromán et al.<sup>7</sup> for Ni-BaTiO<sub>3</sub> is at variance to the trend observed in other work reviewed here, breaking the general rule for extrinsic materials and demonstrating some potential that may require further investigation; this is discussed in detail in the supporting information, Fig. S1. A later study by Saleem et al.<sup>18</sup> on the same composite system is, however, included in Fig. 2 and follows the same trend as the other data sets.

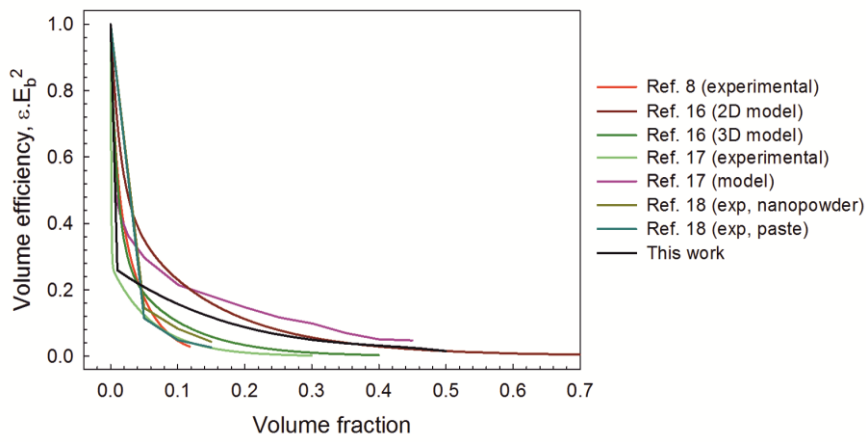


Fig. 2. Energy storage material merit index for energy density,  $\epsilon_r (E_{dielectric})^2$  as a function of conductor volume fraction calculated from curve fitting of data in Fig. 1 normalised to single phase matrix properties of each system.

The data from the literature presented in Fig. 1 and Fig. 2 is supplemented by a 2D electrostatic finite element model (Ansys) we have developed to gain a better understanding of the mechanism behind the observed ‘colossal’ or ‘giant’ permittivity of metal-dielectric composites. A square mesh was divided into 50 x 50 equally sized square elements, which were initially assigned a nominal relative permittivity;  $\epsilon_r = 1$ . ‘Conductive’ elements were selected at random and assigned a permittivity  $10^6$  higher than the matrix. This ensured that the electric field across the ‘conductive’ elements was effectively zero, i.e. the field we would expect across a conductor under equilibrium. An electric field ( $E_{applied}$ ) was applied across the finite element matrix, and the capacitance measured from the stored electrical energy and the maximum local field magnitude ( $E_{max}$ ) recorded. The effective permittivity of the composite was calculated from the capacitance and the normalised effective breakdown strength was predicted from the relationship:

$$E_b^* = \frac{E_{applied}}{E_{max}} \quad \text{Eqn. 6}$$

whereby breakdown was assumed to occur at the point of highest field concentration and cascades onwards from the weakest point. For the filler free matrix the electric field is homogeneous and  $E_{applied} = E_{max}$ ; however, we will see that the introduction of the conductive elements into a dielectric matrix leads to electric field concentrations.

Dielectric breakdown of the composite was assumed to occur in the dielectric phase, as a conductor is effectively in a permanent state of ‘breakdown’, and so the maximum field applied to the composite compared to the matrix as a single phase must be reduced by a concentration factor,  $1/E_{max}$ . This concentration factor enables calculation of the effective breakdown strength,  $E_b^*$ , of the composite. It should be highlighted that the modelling approach ignores the potential of the filler introducing additional defects, which could reduce breakdown strength even further.<sup>19</sup>

Electric field contour plots of models with conductor volume fractions of 0.1, 0.3 and 0.5 are shown in Fig. 3 to demonstrate the influence of conductor additions on the electric field distribution throughout the composite. As the volume fraction of conductive material in the dielectric matrix increases the electric field becomes increasingly more inhomogeneous and the maximum local electric field increases; see the contour maps in Fig. 3. This leads to a reduction in the breakdown strength of the material, which can be seen in the lower trend line in Fig. 1. The electric field concentrations within the matrix act to increase the stored energy due to an applied field, therefore leading to a significant increase in measured effective permittivity, see model data in the upper trend line in Fig. 1. Good agreement is observed between our model and other reported experimental and modelling data. The modelled energy density figure of merit also decreases with increasing conductor fraction, as seen in Fig. 2. For conductor volume fractions  $> 0.4$  the permittivity may be considered ‘colossal’ since the effective permittivity is an order of magnitude higher than that of the matrix. However, there has been no change in the ability of the constituent phases themselves to store more energy, since their permittivities remain constant, and the observed increases in effective permittivity are at the expense of forming areas of high local electric field that significantly reduce the breakdown strength and the energy density figure of merit.

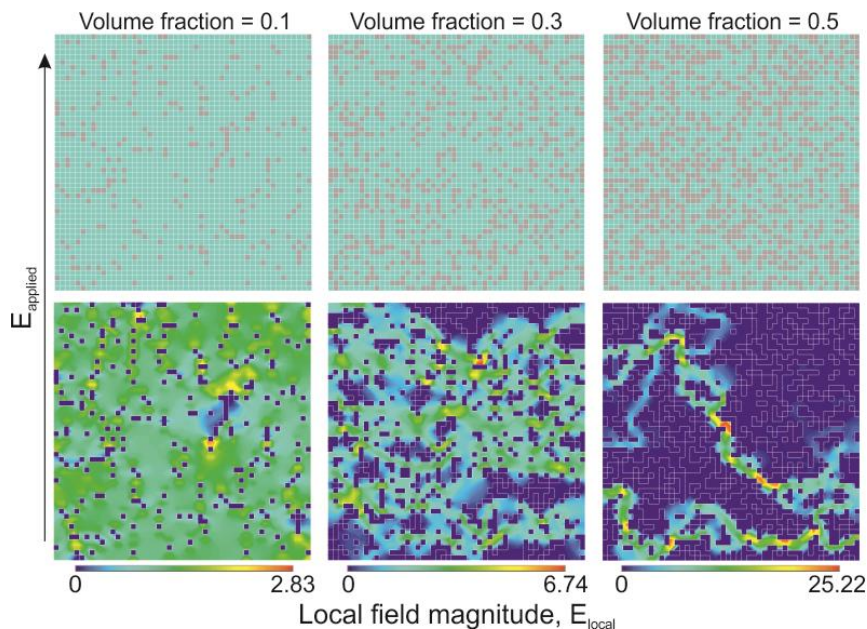


*Figure 3. Finite element model of two phase composites with varying volume fraction of conducting phase. Upper images show example random distributions of conductor (grey) in dielectric matrix (cyan) and lower images are corresponding contour plots*

after application of normalised external electric field ( $E_{\text{applied}} = 1$ ). For a filler free matrix  $E_{\text{local}} = 1$  at all locations.

The network model above is based on a random distribution of equiaxed conductive fillers within a dielectric matrix. One method that has been proposed to reduce electric field concentrations and avoid a reduction in breakdown strength in composites is to alter the aspect ratio and angle of the filler with respect to the direction of the working electric field. In particular, the alignment of high aspect ratio nanofibers perpendicular to the direction of applied field has been considered and has been used in systems containing high permittivity fillers.<sup>20-23</sup> To examine this approach for metal-dielectric composites we now consider a single conductive particle at a fixed volume within a dielectric matrix. We then vary its aspect ratio and orientation ( $\theta$ ) with respect to the applied electric field; when  $\theta = 0^\circ$  the filler particle is aligned parallel to the applied field and when  $\theta = 90^\circ$  the particle is orientated perpendicular to the applied field. Electric field contour maps of these conditions for an aspect ratio of eight are shown in Fig. 4a. The results for the effect of angle and aspect ratio on  $E_b^*$ , normalised permittivity and energy density ( $\epsilon.(E_b^*)^2$ ) are shown in Fig. 4b – d, respectively, calculated using the methods discussed previously. The dashed line in Fig. 4b – d represents the property of the filler free matrix material.

We can see in Fig. 4b that high aspect ratio inclusions aligned perpendicular to the applied field give rise to composites with the highest breakdown strength as this orientation results in the lowest field concentrations, see also Fig 4a. The worst breakdown strength is found when high aspect ratio particles are aligned parallel the applied field. However, whatever the orientation of the conductive filler relative to the applied field, or its aspect ratio, the breakdown strength is always lower than that of the single phase filler-free matrix in which the field is homogenous at all points in the matrix. The opposing trend is observed for the permittivity, Fig. 4c, which is unsurprising since field concentrations are beneficial to the effective permittivity but detrimental to dielectric strength. In this case, the highest permittivity is achieved when high aspect ratio inclusions are aligned parallel to the applied field since this leads to the highest field concentrations. Despite the high permittivity, this composite geometry has the lowest breakdown strength and the volume energy density is significantly reduced (<1%) compared to the matrix, see Fig. 4d. Since the  $\epsilon_r.(E_{\text{dielectric}})^2$  figure of merit for energy density depends on the square of the breakdown strength, the inclusion of conductive fillers of any orientation or aspect ratio reduces the energy storage capabilities of the composite compared to the matrix material, see Fig 4d.



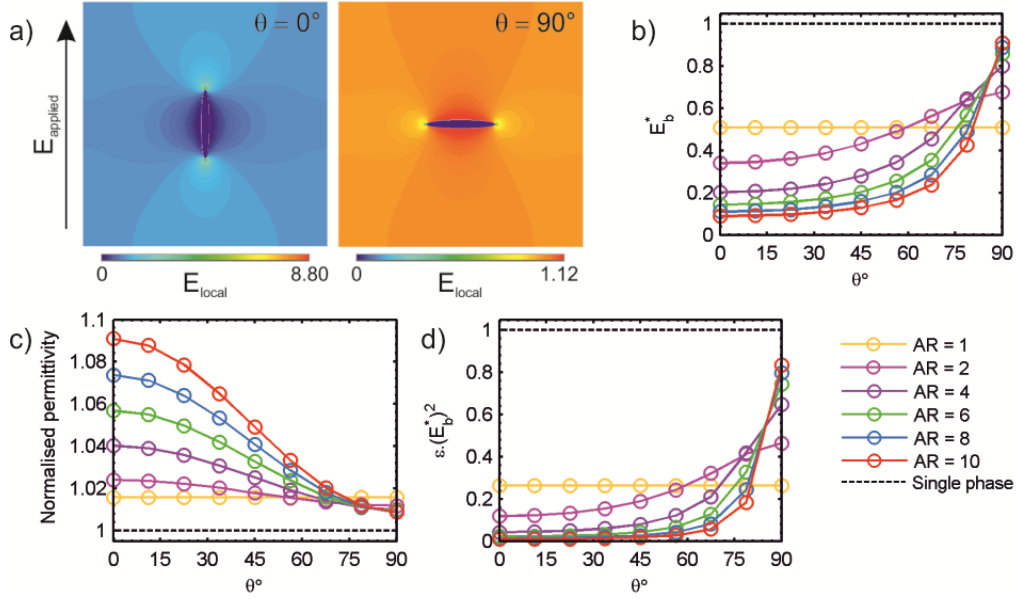


Fig. 4. a) Example contour maps of electric field distribution for an individual conductive inclusion with high aspect ratio ( $AR = 8$ ), and angle with respect to applied field ( $\theta = 0^\circ$  (left) and  $90^\circ$  (right)) contained within a dielectric matrix; and variation of b) effective breakdown strength,  $E_b^2$ , c) permittivity and d) energy density,  $\epsilon_r.(E_{\text{dielectric}})^2$  with changing angle and aspect ratio of single inclusion.

The use of high permittivity fillers in an effort to enhance effective permittivity also leads to similar effects in terms of changes in permittivity and dielectric strength;<sup>20-26</sup> this is due to the high permittivity additions also forming electric field concentrations in the lower permittivity host. Introducing an interphase between matrix and high permittivity filler, through surface functionalisation of the filler<sup>21-25</sup> or using the filler to enhance the crystallisation of the polymer matrix<sup>27</sup> and thereby improve its dielectric strength may provide a route to reducing the problem, although it is unlikely to remove the problem completely as any high permittivity or conductive filler essentially behaves as a defect that leads to field concentrations in the matrix. The use of relatively low permittivity oxide fillers such as  $\text{TiO}_2$ <sup>28</sup> and  $\text{ZrO}_2$ <sup>29</sup> ( $\epsilon_r < 50$ ) with similar permittivity to a ferroelectric polymer matrix have been shown to have higher breakdown strength than nanocomposites with high permittivity fillers;<sup>15</sup> however there appears to be little reward in terms of enhancement of dielectric properties towards giant permittivity.

To conclude, we have shown that extrinsic giant or colossal permittivity materials are unlikely to be candidate materials for multi-layer and small volume high-performance capacitors. Conductive fillers increase the effective permittivity of a conductor-dielectric composite by creating local electric field concentrations within the material. However, these internal electric field enhancements are limited in practice to the magnitude of the breakdown field strength of the filler free dielectric matrix. Consequently, the maximum field that can be applied to the composite, its effective breakdown field strength, will be reduced in magnitude from that of the filler free dielectric matrix. Since the enhanced permittivity in extrinsic materials originates from local internal electric field enhancements, it is impossible to produce composite configurations that achieve a giant permittivity without reducing the effective dielectric strength of the material. In fact, emphasis should be placed on the development of materials with ‘giant’ or ‘colossal’  $\epsilon_r.(E_{\text{dielectric}})^2$  merit index. This work indicates the properties of extrinsic materials, both obtained experimentally and through modelling,



have merit indices that are poorer than the corresponding filler free dielectric matrix materials. Hence it is recommended that the search for genuinely useful giant or colossal dielectric materials is confined to devising means of enhancing the intrinsic dielectric properties of materials.

## Notes

Views expressed in this Viewpoint are those of the authors and not necessarily the views of the ACS.

The authors declare no competing financial interest.

## Acknowledgments

The authors would like to pay tribute to Professor Darryl Almond who passed away before submission of this article. He was a good scientist, a kind man and more. J. I. Roscow would like to acknowledge EPSRC for providing financial support during this research. C. R. Bowen would like to acknowledge funding from the European Research Council under the European Union's Seventh Framework Programme (FP/2007-2013)/ERC Grant Agreement no. 320963 on Novel Energy Materials, Engineering Science and Integrated Systems (NEMESIS).

**Supporting Information Available:** Normalised energy density figures of merit for data from literature including that from Pecharromás et al.<sup>7</sup> excluded from Fig. 2 in the main text with accompanying discussion; curve fitting; additional details for finite element model.

## References

- (1) Hu, W.; Liu, Y.; Withers, R. L.; Frankcombe, T. J.; Norén, L.; Snashall, A.; Kitchin, M.; Smith, P.; Gong, B.; Chen, H.; *et al.* Electron-Pinned Defect-Dipoles for High-Performance Colossal Permittivity Materials. *Nat. Mater.* **2013**, *12*, 821.
- (2) Homes, C. C.; Vogt, T. Colossal Permittivity Materials: Doping for Superior Dielectrics. *Nat. Mater.* **2013**, *12*, 782.
- (3) Li, Z.; Luo, X.; Wu, W.; Wu, J. Niobium and Divalent-Modified Titanium Dioxide Ceramics: Colossal Permittivity and Composition Design. *J. Am. Ceram. Soc.* **2017**, *7*, 3004-3012.
- (4) Du, H.; Lin, X.; Zheng, H.; Qu, B.; Huang, Y.; Chu, D. Colossal Permittivity in Percolative Ceramic/Metal Dielectric Composites. *J. Alloys Compd.* **2016**, *663*, 848-861.
- (5) C. Pecharromás, C.; Moya, J. S. Experimental Evidence of a Giant Capacitance in Insulator-Conductor Composites at the Percolation Threshold. *Adv. Mater.* **2000**, *12*, 294.
- (6) George, S.; James, J.; Sebastian, M. T. Giant Permittivity of a Bismuth Zinc Niobate-Silver Composite. *J. Am. Ceram. Soc.* **2007**, *90*, 3522-3528.
- (7) Pecharromás, C.; Esteban-Betegón, F.; Bartolomé, J. F.; López-Esteban, S.; Moya, J. S. New Percolative BaTiO<sub>3</sub>-Ni ( $\epsilon_r \approx 80000$ ). *Adv. Mater.* **2001**, *13*, 1541-1544.
- (8) Panteny, S.; Bowen, C. R.; Stevens, R. Characterisation of Barium Titanate-Silver Composites part II: Electrical Properties. *J. Mat. Sci.* **2006**, *41*, 3837-3843.

- (9) Huang, J.; Zheng, H.; Chen, Z.; Gao, Q.; Maa, N.; Du, P. Percolative Ceramic Composites with Giant Dielectric Constants and Low Dielectric losses. *J. Mater. Chem.* **2009**, *19*, 3909-3913.
- (10) Huang, X.; Jiang, P.; Xie, L. Ferroelectric Polymer/Silver Nanocomposites with High Dielectric Constant and High Thermal Conductivity. *Appl. Phys. Lett.* **2009**, *95*, 242901.
- (11) Stoyanov, H.; Mc Carthy, D.; Kollosche, M.; Kofod, G. Dielectric Properties and Electric Breakdown Strength of a Subpercolative Composite of Carbon Black in Thermoplastic Copolymer. *App. Phys. Lett.* **2009**, *94*, 232905.
- (12) Luna, A.; Yuan, J.; Neri, W.; Zakri, C.; Poulin, P.; Colin, A. Giant Permittivity Polymer Nanocomposites Obtained by Curing a Direct Emulsion. *Langmuir* **2015**, *31*, 12231-12239.
- (13) Yuan, J. K.; Yao, S.; Dang, Z.; Sylvestre, A.; Genestoux, M.; Bai, J. Giant Dielectric Permittivity Nanocomposites: Realizing True Potential of Pristine Carbon Nanotubes in Polyvinylidene Fluoride Matrix through an Enhanced Interfacial Interaction. *J. Phys. Chem. C* **2011**, *115*, 5515-5521.
- (14) McLean, D. A. Dielectric Materials and Capacitor Miniaturization. *IEEE Trans. Parts, Mater. and Packag.* **1967**, *3*, 163-169.
- (15) Dang, Z.; Yuan, J.; Yao, S.; Liao, R. Flexible Nanodielectric Materials with High Permittivity for Power Energy Storage. *Adv. Mater.* **2013**, *25*, 6334-6365.
- (16) Gyure, M. F.; Beale, P. D. Dielectric Breakdown in Continuous Models of Metal-Loaded Dielectrics. *Phys. Rev. B* **1992**, *46*, 3736-3746.
- (17) P.M.Duxbury, P. M.; Beale, P. D.; Bak, H.; Schroeder, P. A. Capacitance and Dielectric Breakdown of Metal Loaded Dielectrics. *J. Phys. D: App. Phys.* **1990**, *23*, 1546-1553.
- (18) Saleem, M.; Song, J. S.; Jeong, S. J.; Kim, M. S.; Yoon, S.; Kim, I. S. Dielectric Response on Microwave Sintered BaTiO<sub>3</sub> Composite with Ni Nanopowder and Paste. *Mater. Res. Bull.* **2015**, *64*, 380-385.
- (19) Li, J. Y.; Zhang, L.; Duchame, S. Electric Energy Density of Dielectric Nanocomposites. *Applied Physics Letters* **2007**, *90*, 132901.
- (20) Tang, H. X. Nanocomposites with Increased Energy Density through High Aspect Ratio PZT Nanowires. *Nanotech.* **2011**, *22*, 015702.
- (21) Wang, S.; Huang, X.; Wang, G.; Wang, Y.; He, J.; Jiang, P. Increasing the Energy Efficiency and Breakdown Strength of High-Energy-Density Polymer Nanocomposites by Engineering the Ba<sub>0.7</sub>Sr<sub>0.3</sub>TiO<sub>3</sub> Nanowire Surface via Reversible Addition-Fragmentation Chain Transfer Polymerization. *J. Phys. Chem. C* **2015**, *119*, 25307-25318.
- (22) Zhang, X.; Chen, W.; Wang, J.; Shen, Y.; Gu, L.; Lin, Y.; Nan, C.-W. Hierarchical Interfaces Induce High Dielectric Permittivity in Nanocomposites Containing TiO<sub>2</sub>@BaTiO<sub>3</sub> Nanofibers. *Nanoscale* **2014**, 6701-6709.
- (23) Liu, S.; Zhai, J. Improving the Dielectric Constant and Energy density of Poly(Vinylidene Fluoride) Composites Induced by Surface-Modified SrTiO<sub>3</sub> Nanofibers by Polyvinylpyrrolidone. *J. Mater. Chem. A* **2015**, *3*, 1511-1517.
- (24) Zhang, X.; Shen, Y.; Zhang, Q.; Gu, L.; Hu, Y.; Du, J.; Nan, C. W. Ultrahigh Energy Density of Polymer Nanocomposites Containing BaTiO<sub>3</sub>@TiO<sub>2</sub> nanofibers by atomic-scale interface engineering. *Adv. Mater.* **2015**, *27*, 819.

- (25) Liu, S. H. Surface-Modified Ba(Zr<sub>0.3</sub>Ti<sub>0.7</sub>)O<sub>3</sub> Nanofibers by Polyvinylpyrrolidone Filler for Poly(Vinylidene Fluoride) Composites with Enhanced Dielectric Constant and Energy Storage Density. *Sci. Rep.* **2016**, *6*, 26198.
- (26) Tang, H.; Sodano, H. A. Ultra High Energy Density Nanocomposite Capacitors with Fast Discharge Ba<sub>0.2</sub>Sr<sub>0.8</sub>TiO<sub>3</sub> nanowires. *Nano Lett.* **2013**, *13*, 1373-1379.
- (27) Luo, H.; Roscow, J.; Zhou, X.; Chen, S.; Han, X.; Zhou, K.; Bowen, C. Ultra-High Discharged Energy Density Capacitor using High Aspect Ratio Na<sub>0.5</sub>Bi<sub>0.5</sub>TiO<sub>3</sub> Nanofibers. *J. Mater. Chem. A* **2017**, *5*, 7091-7102.
- (28) Li, J.; Seok, S.; Chu, B.; Dogan, F.; Zhang, Q.; Wang, Q. Nanocomposites of Ferroelectric Polymers with TiO<sub>2</sub> Nanoparticles Exhibiting Significantly Enhanced Electrical Energy Density. *Adv. Mater.* **2009**, *21*, 217-221.
- (29) Zou, C.; Kushner, D.; Zhang, S. Wide Temperature Polyimide/ ZrO<sub>2</sub> Nanodielectric Capacitor Film with Excellent Electrical Performance. *Appl. Phys. Lett.* **2011**, *98*, 082905.